




# APPLICATION OF NEURAL NETWORK REGRESSION FOR DENSITY LOG CONSTRUCTION: COMPARISONS WITH TRADITIONAL EMPIRICAL MODELS

Caique P. Carvalho <sup>1</sup>, Carolina B. da Silva <sup>1</sup>,  
José Jadsom S. de Figueiredo <sup>1,2</sup>, and Mayra D. L. Carrasquilla

<sup>1</sup>Universidade Federal do Pará–UFPA, Faculty of Geophysics, Petrophysics and Rock Physics Laboratory, Belém, PA, Brazil

<sup>2</sup>National Institute of Petroleum Geophysics (INCT-GP), Brazil

\*Corresponding author: [caique.pc94@gmail.com](mailto:caique.pc94@gmail.com)

**ABSTRACT.** Determination of the reflection coefficients is a key element to a well to seismic tie, and the density log has great petrophysical importance as it is used to calculate the acoustic impedance and the reflectivity log. Many authors have developed empirical relations to determine the bulk density log from other log information such as compressional velocity and shale volume fraction. However, as machine learning (ML) techniques have advanced, many works have used them to solve problems involving regression and classification in well log data. The primary goal of this study is to develop Artificial Neural Network (ANN) regression models which predict the density log and use other logs as input, and then compare them to existing empirical models and find out which one provides the best fit. Two ANN models were developed, and a statistical analysis was used to compare both to empirical models, such as calculating the mean squared error, relative error, and correlation factor. When compared to empirical models, both ANN models had smaller errors and higher precision on the fit.

**Keywords:** artificial neural networks, well logging, petrophysics

## INTRODUCTION

The density log plays a major role both in well logging and in well to seismic tying. Its importance is due to the petrophysical information that can be determined by the rock densities and applied to the oil and gas industry. A formation evaluation can be constructed utilizing the density log associated with other log information. By calculating the acoustic impedance of the medium, which results from the product of the density and the P-wave velocity, it is possible to calculate the seismic reflection coefficients which are fundamental in the well to seismic tie. From laboratory studies containing sedimentary samples of different basins, geological ages, and depths, [Gardner et al. \(1974\)](#) developed an empirical equation that calculates the density from the P-wave velocity information, also allowing the calculation of acoustic impedance and seismic reflection coefficients from the P-wave velocity information alone.

Besides [Gardner et al. \(1974\)](#), other authors,

[Brocher \(2005\)](#), [Lindseth \(1979\)](#), [Christensen and Mooney \(1995\)](#), and [Birch \(1960\)](#) developed empirical equations to calculate the density log. Two important empirical models were proposed by [Oloruntobi and Butt \(2019\)](#), which consider for the calculation of the density log not only the P-wave velocity information ( $V_P$ ) but also the volume fraction of shale ( $V_{sh}$ ). The first model is a linear equation obtained by modifying the equation of [Han et al. \(1986\)](#). The second model was obtained from Gardner's equation in which the term for the volume fraction of shale was added. The equation parameters were calculated in the article utilizing core samples from USA and Gulf of Mexico wells, but they can also be calculated for other formations utilizing a linear regression method for the first model and a non-linear regression method for the second one. A special focus will be given to the empirical equation of [Gardner et al. \(1974\)](#) and to the second empirical model of [Oloruntobi and Butt \(2019\)](#) because these equations were developed for sedimen-

tary formations and present small errors in the density log calculation.

Nowadays, the use of Artificial Intelligence (AI) and Machine Learning (ML) in geophysics has become frequent and it will be indispensable in the near future. Artificial Neural Networks (ANNs), which are a sub-branch of the ML, were first developed by [McCulloch and Pitts \(1943\)](#) as a mathematical model and then evolved with the works of authors like [Hebb \(1949\)](#), [Rochester et al. \(1956\)](#), [Rosenblatt \(1958\)](#), [Widrow \(1960\)](#). The applications of Artificial Neural Networks are very broad. For instance, they might be found in medical diagnostics, voice recognition, fraud detection, and many others. Geophysical applications can be found in the works of [Kohli and Arora \(2014\)](#), [Long et al. \(2016\)](#), which are well logging applications, [Van der Baan and Jutten \(2000\)](#), and [Zeng et al. \(2022\)](#). A problem that arises in the construction of the density log utilizing empirical equations, either with the original parameters calculated by the authors or by re-calibrating them with linear or nonlinear regressions for specific formations, is that the error between real and calculated density logs might be significant due to geological factors as geochronological differences in the formations and fractured rocks. As an attempt to overcome this issue, an Artificial Neural Network algorithm will be used to create models that construct the density log by having other geophysical logs as input data. The results of the ANN models will be compared with the results from the empirical equations to determine which one presents the best adjustment.

## THEORETICAL BACKGROUND

The comparison between the empirical models and the Artificial Neural Networks models in this work was performed in two separate ways. The first comparison was between the ANN models and the empirical models with their original parameter values from the articles. The second comparison was between the ANN models and the empirical models with new parameter values calculated by inversion utilizing a reference well. The optimization methods utilized in the inversion and also in the ANN algorithm are described below.

### The least squares method

The theory of least squares was developed by Carl Friedrich Gauss ([Stigler, 1981](#)). It is a numerical analysis method in which a group of functions and a set of variables (both dependent and independent) are provided to determine the best fit of a continuous function with the variables data by the criterion of minimum square error ([Leon et al., 1998](#)). To attempt to find a set of coefficients  $c_i$  (where  $i=1,2,3,\dots,n$ ),  $f(x)$  interpolates with the set  $\{(x_j, y_j)\}_{j=1}^n$  - being  $(x_j, y_j)$  a set of points in the Cartesian plane - which can be

represented by:

$$\sum_{i=1}^m c_i f_i(x_j) = y_j, \quad (1)$$

where equation (1) written in a matrix structure is:

$$\begin{bmatrix} f_1(x_1) & f_2(x_1) & \dots & f_i(x_1) \\ f_1(x_2) & f_2(x_2) & \dots & f_i(x_2) \\ \vdots & \vdots & \vdots & \vdots \\ \vdots & \vdots & \vdots & \vdots \\ f_1(x_n) & f_2(x_n) & \dots & f_i(x_n) \end{bmatrix} \begin{bmatrix} c_1 \\ c_2 \\ \vdots \\ \vdots \\ c_m \end{bmatrix} = \begin{bmatrix} y_1 \\ y_2 \\ \vdots \\ \vdots \\ y_n \end{bmatrix}, \quad (2)$$

which can be rewritten as:

$$Mc = y, \quad (3)$$

where M is the matrix containing the functions' outputs for each  $x_j$  and c is the vector containing the adjustable parameters. According to [Kailath \(1980\)](#), to find a solution, the first step is to multiply both sides by the transverse matrix of M:

$$M^T Mc = M^T y. \quad (4)$$

The following step is to multiply both sides by  $[M^T M]^{-1}$  and obtain the solution for c:

$$c = [M^T M]^{-1} M^T y. \quad (5)$$

The least squares method will be utilized to calculate the parameters of [Gardner et al. \(1974\)](#) equation by inversion for a reference well.

### The Levenberg-Marquardt method

The Levenberg-Marquardt method ([Levenberg, 1944](#); [Marquardt, 1963](#)) can be derived from Newton's method:

$$\mathbf{x}^{(s+1)} = \mathbf{x}^{(s)} - (\mathbf{A}^{(s)})^{-1} \mathbf{g}^{(s)}, \quad (6)$$

where  $\mathbf{A}^{(s)}$  is the Hessian matrix  $\mathbf{A}^{(s)} = \nabla^2 F(\mathbf{x})$  and  $\mathbf{g}^{(s)}$  is the gradient. It is possible to make approximations for the Hessian matrix:

$$\nabla^2 F(\mathbf{x}) \cong \mathbf{J}^T(\mathbf{x})\mathbf{J}(\mathbf{x}), \quad (7)$$

and for the gradient:

$$\nabla F(\mathbf{x}) \cong \mathbf{J}^T(\mathbf{x})\mathbf{r}(\mathbf{x}^{(s)}), \quad (8)$$

and replacing equations 7 and 8 in equation 6, it is possible to obtain the Gauss-Newton method:

$$\mathbf{x}^{(s+1)} = \mathbf{x}^{(s)} + (\mathbf{J}^T \mathbf{J})^{-1} \mathbf{J}^T \mathbf{r}(\mathbf{x}^{(s)}), \quad (9)$$

where  $\mathbf{J}$  is the Jacobian matrix and  $\mathbf{r}$  is the error associated with the function values. According to Kayri (2016) it is necessary to add Levenberg's damping factor  $\mu$ , multiplied by the identity matrix to regularize the Gauss-Newton method when the product:  $(\mathbf{J}^T \mathbf{J})$  results in a singular matrix and thus arrive at the Levenberg-Marquardt equation:

$$\mathbf{x}^{(s+1)} = \mathbf{x}^{(s)} + (\mathbf{J}^T \mathbf{J} + \mu \mathbf{I})^{-1} \mathbf{J}^T \mathbf{r}(\mathbf{x}^{(s)}), \quad (10)$$

The Jacobian matrix is composed of the first partial derivatives:

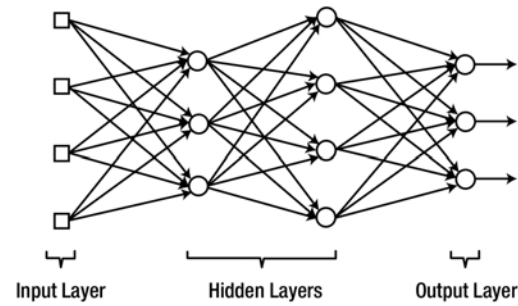
$$\mathbf{J} = \begin{bmatrix} \frac{\partial r_1}{\partial x_1} & \cdots & \frac{\partial r_1}{\partial x_n} \\ \vdots & \ddots & \vdots \\ \frac{\partial r_m}{\partial x_1} & \cdots & \frac{\partial r_m}{\partial x_n} \end{bmatrix}. \quad (11)$$

On equation 10,  $\mathbf{x}^{(s+1)}$  is the updated  $\mathbf{x}$  value,  $\mathbf{x}^{(s)}$  is the previous  $\mathbf{x}$  value. The damping factor  $\mu$  leads to optimization and, depending on its value, the Levenberg-Marquardt algorithm can become the steepest descent method. The Levenberg-Marquardt is utilized in this work to re-calculate the parameters of modified Gardner's equation of Olorunjobi and Butt (2019) by inversion for the reference well. It is also utilized in the ANN algorithm as an optimization method to update the weights of the network.

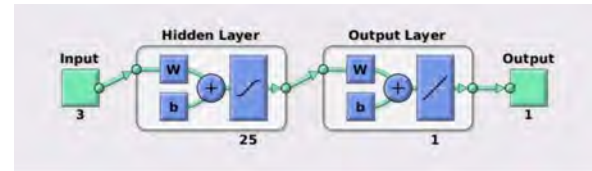
## Artificial Neural Networks

The different types of ML are supervised learning, unsupervised learning, and reinforcement learning. A supervised learning algorithm will be applied consisting of feeding the network with input and correct output (target) pairs. The mean squared error will be calculated at each iteration between the correct output values and the output values at that iteration, followed by a weight update so that the mean squared error decreases in the following iterations until a minimum value is reached and the training stops. The optimum values reached for the weights and biases will compose the created ANN model.

The ANN were first developed by McCulloch and Pitts (1943) as a mathematical model to simulate a biological neuron. The pioneer ANN model was the Perceptron developed by Rosenblatt (1958), which consisted of a very simple model with one input/output artificial neuron. Modern ANNs consist of multiple layer networks as shown in Figure 1a, with one input layer, one output layer, and some hidden layers. The ANN algorithm developed in this work consists of one input layer, one hidden layer, and one output layer. The network has a total of 25 neurons in its hidden layer and 1 neuron in its output layer. Its architecture is represented in Figure 1b.



(a) Multiple layer network.



(b) NNSTART Architecture.

Figure 1: (a) Diagram of a multi-layer network architecture. On the left there is the input layer, followed by the hidden layers and output layer. Each circle represents an artificial neuron (Kim, 2017). (b) Neural network architecture of the NNSTART MATLAB function used in this work. The hidden layer contains 25 neurons and the output layer contains 1 neuron. Adapted from Beale et al. (2010).

The mathematical model for a single layer ANN is given by:

$$Y_k = f(W_{km} X_m + B_k), \quad (12)$$

where  $W_{km}$  is the matrix containing the weights of the neural network that will be multiplied with the input vector ( $X_m$ ) and then summed with the bias vector ( $B_k$ ). The result of this operation is the input for the activation function  $f$  and gives the calculated output vector  $Y_k$ . Also, we can use different notation for equation 12, which individually calculates each element  $y_i$  of vector  $Y_k$  individually as given by:

$$y_i = f \left( \sum_{j=1}^m w_{i,j} x_j + b_i \right), i = 1, 2, 3 \dots k. \quad (13)$$

The matrix multiplication in details will be:

$$Y_k = f \left[ \begin{bmatrix} w_{11} & w_{12} & \cdots & w_{1m} \\ w_{21} & w_{22} & \cdots & w_{2m} \\ \vdots & \vdots & \ddots & \vdots \\ w_{k1} & w_{k2} & \cdots & w_{km} \end{bmatrix} * \begin{bmatrix} x_1 \\ x_2 \\ \vdots \\ x_m \end{bmatrix} + \begin{bmatrix} b_1 \\ b_2 \\ \vdots \\ b_k \end{bmatrix} \right]. \quad (14)$$

A variety of activation functions are utilized in ANNs, for example: the sigmoid and rectified linear functions (Menon et al., 1996; Hara et al., 2015). Both were applied in this work, the sigmoid function

on the hidden layer and a linear transfer function on the output layer. To update the weights, it is necessary to utilize an optimization method. In this work, the Levenberg-Marquardt backpropagation method is utilized and is represented on equation 10.

## METHODOLOGY

The main goal of this work is to construct a pseudo density log based on ANN models and compare them with the empirical equations. It is possible to observe in Figure 2 all the steps of the work that lead to the best fit selection. The empirical equations utilized in this work are listed in the following section. The point is to test each equation for well logs of different sedimentary basins and analyze their limitations by calculating the relative error (R.E), the mean squared error (M.S.E), the root mean squared error (R.M.S.E), an adjustment factor (R) between the real density log and the density log calculated by the empirical equation and comparing them with the results from the ANN models.

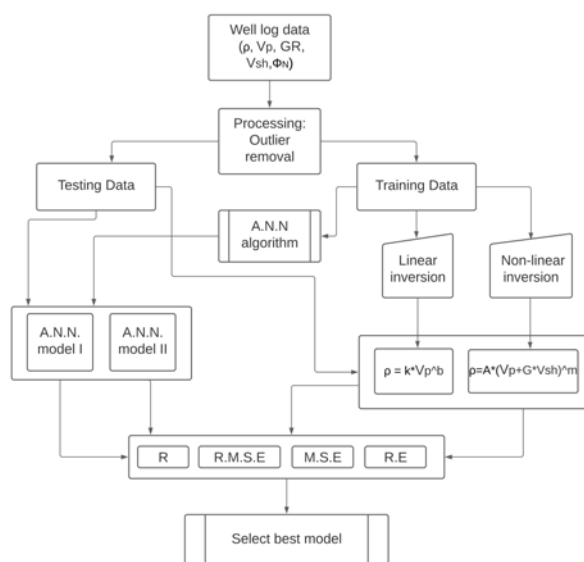


Figure 2: Illustration of the flowchart detailing the steps of the work methodology.

The function NNSTART (Neural Network Start) from the MATLAB programming language is utilized to obtain the ANN models (Beale et al., 2010). The dataset utilized to perform the training, validation and testing steps of the ANN contains well log information from the Campos Basin in Brazil, the Norne field in Norway, the Taranaki Basin in New Zealand, and some well logs from Alaska, USA. A second dataset containing well logs from the Penobscot field in Nova Scotia, Canada, was exclusively utilized to perform additional tests. All the well log data were first submitted to an outlier removal phase, as shown in Figure 2, utilizing a despiking function, and then submitted to the steps of the empirical equations and machine learning algorithm. The re-calibration

of the empirical equations' parameters by inversion was made utilizing a reference well from the Norne field.

## Empirical models

The parameters  $k$  and  $B$  for Gardner's equation on its original article, for a P-wave velocity measured in km/s, and bulk density in g/cm<sup>3</sup>, are equal to 1.74 and 0.25, respectively. These parameters can also be obtained by linear regression for other sedimentary basins utilizing the least squares method; nevertheless, the values are generally different. The parameters  $A$ ,  $G$ , and  $m$  for Oloruntobi and Butt (2019) model II, also known as the modified Gardner's model, are equal to 1.350, 1.651, and 0.390, respectively. They can also be obtained for other formations by non-linear regression utilizing the Levenberg-Marquardt method (Levenberg, 1944; Marquardt, 1963) but the values will also be different from the original article ones.

Gardner et al. (1974) equation is given by:

$$\rho_b = k [V_P]^B, \quad (15)$$

where  $\rho_b$  is the bulk density,  $V_P$  is P-wave velocity, and  $k$  is equal to 1.74 and  $B$  is equal to 0.25.

By applying the natural logarithm on both sides of equation 15, a linear equation is obtained. It is now possible to find a solution for the constants  $k$  and  $B$  utilizing the least squares method. Modifying equation 15 with the natural logarithm and applying to equation 2, it is obtained:

$$\begin{bmatrix} 1 & \ln(V_{p1}) \\ 1 & \ln(V_{p2}) \\ \vdots & \vdots \\ 1 & \ln(V_{pn}) \end{bmatrix} \begin{bmatrix} \ln(k) \\ B \end{bmatrix} = \begin{bmatrix} \ln(\rho_{b1}) \\ \ln(\rho_{b2}) \\ \vdots \\ \ln(\rho_{bn}) \end{bmatrix}. \quad (16)$$

Now it is possible to get the values of the vector  $c$ , which is  $c = [\ln(k), b]$  for equation 15 by replacing each element of equation 16 in equation 5. Considering that  $\ln(k) = x_r$ , then it is possible to find the value of  $k$  by applying the exponential function to both sides  $k = \exp(x_r)$ . After these steps, it was possible to obtain the new values for parameters  $k$  and  $B$  utilizing the reference well from the Norne field. As mentioned earlier, the other equation used was the Oloruntobi and Butt (2019). This equation was modified from Gardner's equation. Mathematically, it is given by:

$$\rho_b = A [V_p + G V_{sh}]^m. \quad (17)$$

where  $V_{sh}$  is the shale volume log. The  $V_{sh}$  was calculated from the gamma-ray ( $GR$ ) log utilizing Clavier

et al. (1971) equation:

$$V_{sh} = 1.7\sqrt{3.38 - (I_{GR} + 0.7)^2}, \quad (18)$$

where  $I_{GR}$  is the gamma-ray index given by:

$$I_{GR} = \frac{GR_{log} - GR_{min}}{GR_{max} - GR_{min}}. \quad (19)$$

Here, the Levenberg-Marquardt algorithm was utilized for the regularization of the non-linear inversion of the equation (17) as well as for the regularization of the weights during the training stage of the NN models (it will be discussed later). It is important to point out that, in neural network models, the Jacobian matrix of regularization is composed of the partial derivatives of the function concerning the weights, as shown in equation 24. The Jacobian matrix of the modified Gardner's model is composed of the function derivatives for the parameters A, G, and m:

$$\mathbf{J} = \begin{bmatrix} \frac{\partial \rho_1}{\partial A} & \frac{\partial \rho_1}{\partial G} & \frac{\partial \rho_1}{\partial m} \\ \vdots & \vdots & \vdots \\ \frac{\partial \rho_n}{\partial A} & \frac{\partial \rho_n}{\partial G} & \frac{\partial \rho_n}{\partial m} \end{bmatrix}_{n \times 3}, \quad (20)$$

where  $\frac{\partial \rho_n}{\partial A}$ ,  $\frac{\partial \rho_n}{\partial G}$  and  $\frac{\partial \rho_n}{\partial m}$  are the partial derivatives of the function with respect to the parameters. When the parameters k and B from the traditional Gardner's equation, and also the parameters A, G, and m, from the modified Gardner's equation, were calculated by inversion utilizing the first dataset, consisting of well logs from Campos, Norne, Alaska, and Taranaki Basins, their values were very close to the ones of their respective original articles. Therefore, a single well from the Norne field was chosen to be the reference well.

### ANN models

Lv et al. (2017) show that for a NN with two layers, the ANN architecture will be represented by:

$$a^2 = f^2 \left( \sum_{i=1}^S w_{1,i}^2 f^1 \left( \sum_{j=1}^R w_{i,j}^1 p_j + b_i^1 \right) + b^2 \right), \quad (21)$$

which was also the one utilized in this work. For it,  $w_{i,j}^1$ ,  $p_j$ ,  $b_i^1$  and  $f^1$  represent the weights, input vector, bias, and activation function for the hidden layer; R is the size of the input vector  $p_j$ , while  $w_{1,i}^2$ ,  $b^2$ , and  $f^2$  represent the weights, bias, and activation function for the second layer (output layer);  $a^2$  represents the network output. The input data might also be a matrix. However, to establish the matrix multiplication, the number of columns of the matrix containing the weights needs to be equal to the number of lines of the input matrix. This also guarantees that each weight value is associated with each input value. It is important to notice in equation 21 that there is

an inner equation similar to equation 13 which represents the outputs of the first layer. Each of these elements is multiplied by the weights of the second layer and then summed, showing that the outputs of the first layer are inputs of the second layer. The next steps after the training of the ANN will be validating and testing. Table 1 shows the total number of samples from the data utilized for both ANN models and how they were split: 80 % for training, 10 % for validation, and 10 % for testing. Additional tests were made with the second dataset containing a well log from the Penobscot field in Canada which was used to perform tests on rocks with different lithology, also called "blind tests".

Table 1: Number of samples for the first and second ANN models and percentage used for each step.

	Model 1		Model 2	
	Samples	%	Samples	%
Total	69669	100	35034	100
Training	55735	80	24524	80
Validation	6967	10	5255	10
Testing	6967	10	5255	10

The data from the Campos, Norne, and Penobscot fields were also used to train and build the second neural network model, which was fed with P-wave velocity ( $V_P$ ), gamma-ray ( $GR$ ), and neutron porosity ( $\phi_N$ ) logs. It is important to divide the data for each step of the work. Additional tests were made with well logs from Norne, Norway, and the Campos Basin, Brazil.

The logs used as input data for the first ANN model were the P-wave velocity ( $V_P$ ), calculated from the sonic log (DT), and the volume fraction of shale ( $V_{sh}$ ), calculated from the gamma-ray log ( $GR$ ). In the case of the second model, the neutron porosity log ( $\phi_N$ ) was added as an input. The input to the first and second ANN models is a matrix with two lines (or three lines for the second model) and n rows, with each line representing a log of  $V_P$  and  $V_{sh}$  (and an additional  $\phi_N$  log for the second model). Mathematically this specific architecture is given by:

$$a^2 = f^2 \left( \sum_{i=1}^{25} w_{1,i}^2 f^1 \left( \sum_{j=1}^{2 \text{ or } 3} w_{i,j}^1 p_{jk} + b_i^1 \right) + b^2 \right), \quad (22)$$

$k = 1, 2 \dots n.$

The ideal number of neurons on the hidden layer was reached after several tests that confirmed that many neurons larger than 25 would overfit the model. The density log ( $\rho_b$ ) was used as the target data in both cases. When the training, validation, and test-

ing steps were complete, the final values of weights and biases were stored in a model that will be used to perform new tests.

Figure 3 shows an example of the well log data utilized as input for both ANN models as well as their units of measure. Figure 4 shows the MATLAB NNSTART function User Interface which provides information such as the algorithm utilized to train the network, how the data were split, the number of iterations and validation checks, and the parameter utilized to improve the performance of the network training, which was the mean squared error.

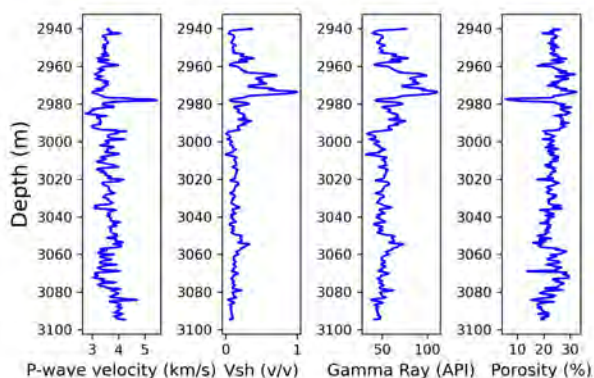


Figure 3: Example of the logs used as input for the ANN models. P-wave velocity and shale volume fraction ( $V_{sh}$ ) for the first model, and P-wave velocity, Gamma ray and Neutron porosity for the second model.

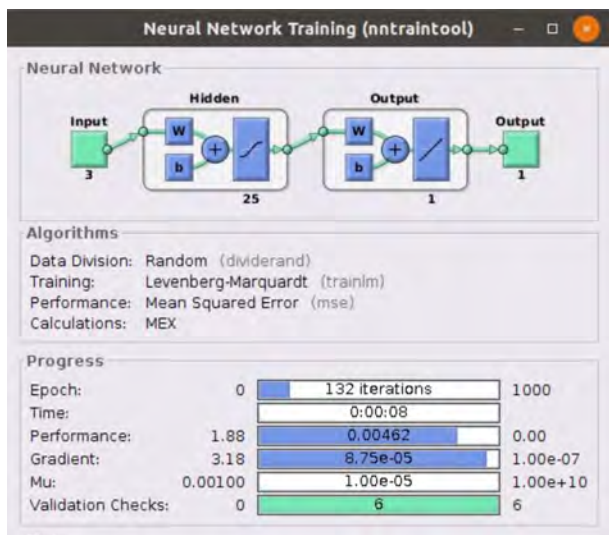


Figure 4: NNSTART User Interface detailing the training and performance of the algorithm. Adapted from Beale et al. (2010).

The Levenberg-Marquardt method was also utilized in the ANN algorithm to optimize the solution for the weight values. The algorithm utilized for neural networks is called Levenberg-Marquardt back-

propagation. Modifying equation 10 for the weight update gives:

$$w^{l+1} = w^l - [\mathbf{J}^T \mathbf{J} + \mu \mathbf{I}]^{-1} \mathbf{J}^T \mathbf{e}. \quad (23)$$

The Jacobian matrix will be:

$$J = \begin{bmatrix} \frac{\partial e_1(w)}{\partial w_1} & \frac{\partial e_1(w)}{\partial w_2} & \dots & \frac{\partial e_1(w)}{\partial w_n} \\ \frac{\partial e_2(w)}{\partial w_1} & \frac{\partial e_2(w)}{\partial w_2} & \dots & \frac{\partial e_2(w)}{\partial w_n} \\ \vdots & \vdots & \ddots & \vdots \\ \frac{\partial e_N(w)}{\partial w_1} & \frac{\partial e_N(w)}{\partial w_2} & \dots & \frac{\partial e_N(w)}{\partial w_n} \end{bmatrix} \quad (24)$$

For the comparison of the empirical equations of the traditional and modified Gardner models (Gardner et al., 1974; Olorunfemi and Butt, 2019) with both ANN models that generate the density log, two types of tests were conducted. The first test consisted of comparing the MSE of the ANN model with the MSE of the traditional and modified Gardner equations, utilizing the original parameter values from the articles. The second test consisted of comparing the ANN model with the traditional and modified Gardner models, in which the parameters were calculated in a well log from a different field, utilizing linear and non-linear regression.

## RESULTS

The regression fit obtained during the training, validation, and testing steps of the ANN algorithm is shown in Figure 5. The adjustments of the density calculated by the empirical equations and the density obtained by the ANN are depicted in Figure 6a. The blue curve is the real density, the red curve is the density calculated by the empirical equation and the black curve is the density calculated by the ANN model. Table 2 shows the values of the mean squared error (MSE) and the Pearson's Correlation Coefficient (R) obtained during the training, validation, and testing steps of the ANN algorithm while creating the first and the second ANN models.

Table 3 shows the mean squared errors for the ANN, the empirical models of Gardner et al. (1974) and Olorunfemi and Butt (2019), while Table 4 shows the correlation factors for the same data.

For the dataset composed of a well log from Campos Basin and another from Penobscot field, tests were performed using the first ANN model. The adjustment is shown in Figures 6a and 6b. The mean squared errors for the different models are displayed in Table 3. The mean squared error between the real density and the density calculated by the ANN model for a Campos Basin well log was 0.0097, while the mean squared error for the same field but with the traditional Gardner equation utilizing the parameters k and B from Gardner et al. (1974) was 0.0147, as shown in Figure 6a. When the parameters k and B were calculated on a well log from the Norne field and

applied to the Campos Basin, the mean squared error was 0.0260, as shown in Figure 6b.

Figure 7a shows the adjustment for the Penobscot field data comparing the ANN model with the traditional Gardner’s equation. The ANN model had a mean squared error of 0.0074 while the traditional Gardner’s equation had a mean squared error of 0.0105. When the parameters k and B were calculated on the Norne field, Gardner’s equation performed worse, showing a mean squared error of 0.0254, which is also greater than the error presented by the ANN. The adjustment is shown in Figure 7b.

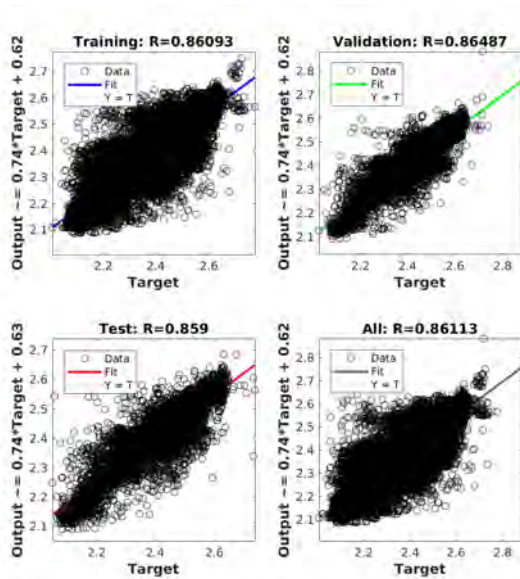


Figure 5: Example of a regression fit during training, validation and testing.

Table 2: Number of samples, Mean Squared Error and Pearson’s Correlation Coefficient R for both ANN models.

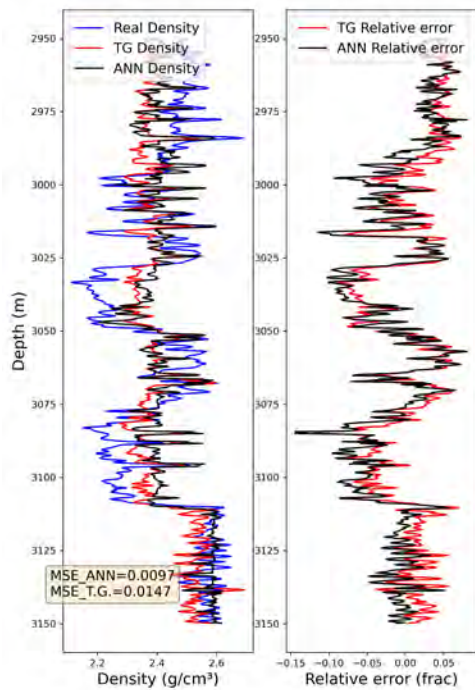
Model 1			
	Samples	MSE	R
Training	55735	0.00421	0.86092
Validation	6967	0.00413	0.86487
Testing	6967	0.00438	0.85900
Model 2			
	Samples	MSE	R
Training	24524	0.00455	0.8874
Validation	5255	0.00492	0.8800
Testing	5255	0.00430	0.8958

Table 3: Mean Squared Error (MSE) for well data from the Campos Basin and for a well from the Penobscot field. A.V. refers to the parameter values from their respective original article while INV refers to the parameters calculated by inversion in a Norne field dataset.

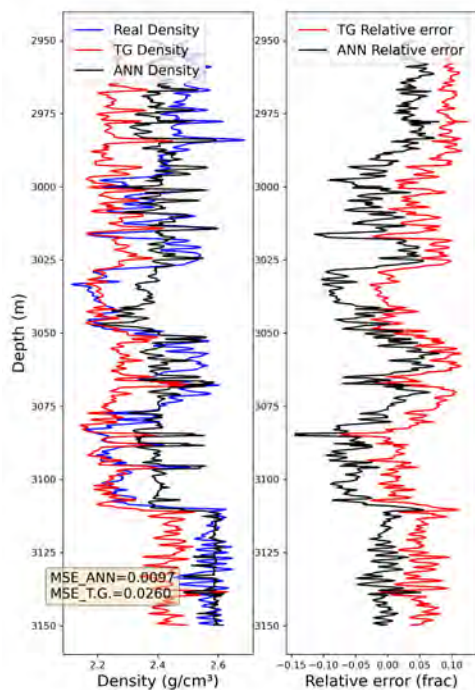
Model	MSE (Campos Basin)	MSE (Penobscot Basin)
Traditional Gardner (A.V.)	0.0147	0.0105
Modified Gardner (A.V.)	0.0209	0.0105
Traditional Gardner (INV)	0.0260	0.0254
Modified Gardner (INV)	0.0355	0.0099
ANN	0.0097	0.0074

Table 4: Pearson’s Correlation Coefficient (R) for well data from the Campos Basin and for a well from the Penobscot field. A.V. refers to the parameter values from their respective original article while INV refers to the parameters calculated by inversion in a Norne field dataset.

Model	MSE (Campos Basin)	MSE (Penobscot Basin)
Traditional Gardner (A.V.)	0.89	0.72
Modified Gardner (A.V.)	0.84	0.64
Traditional Gardner (INV)	0.87	0.72
Modified Gardner (INV)	0.29	0.63
ANN	0.92	0.74

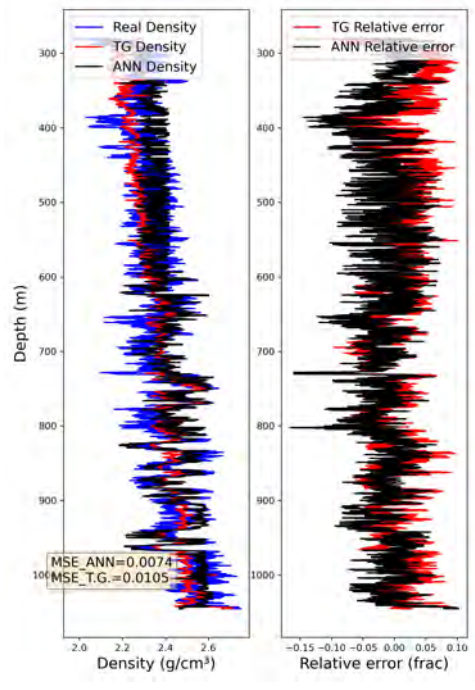


(a) Traditional Gardner (A.V.).

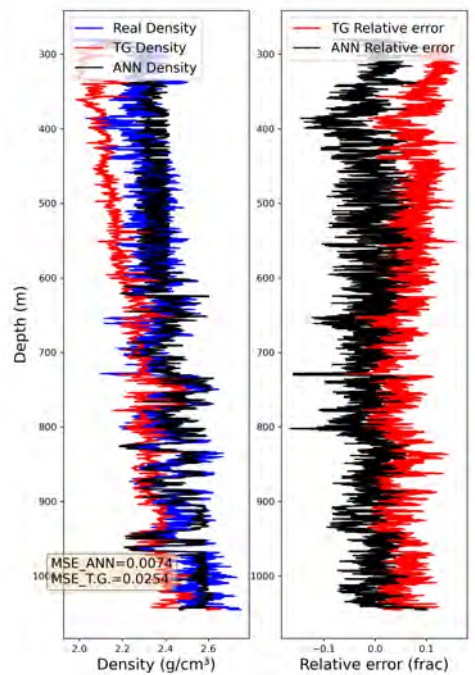


(b) Traditional Gardner (INV).

Figure 6: Comparison between the fit of the density log constructed with the ANN and the traditional Gardner model. (a) It is the comparison of the Gardner model with its original article parameter values (A.V.), represented by the red curve on the plot, and the density log constructed by the ANN model (black curve). (b) It is the comparison of the Gardner model with its parameter values calculated in a Norne field well log by inversion (INV), represented by the red curve on the plot, and the density log constructed by the ANN model (black curve). Both are applied in a Campos Basin dataset.



(a) Traditional Gardner (A.V.).



(b) Traditional Gardner (INV).

Figure 7: Comparison between the fit of the density log constructed with the ANN and the traditional Gardner model. (a) It is the comparison of the Gardner model with its article parameter values (A.V.), represented by the red curve on the plot, and the density log constructed by the ANN model (black curve). (b) It is a comparison of the Gardner model with its parameter values calculated in a Norne field well log by inversion (INV), represented on the plot by the red curve, and the density log constructed by the ANN model (black curve). Both are applied in the Penobscot dataset.



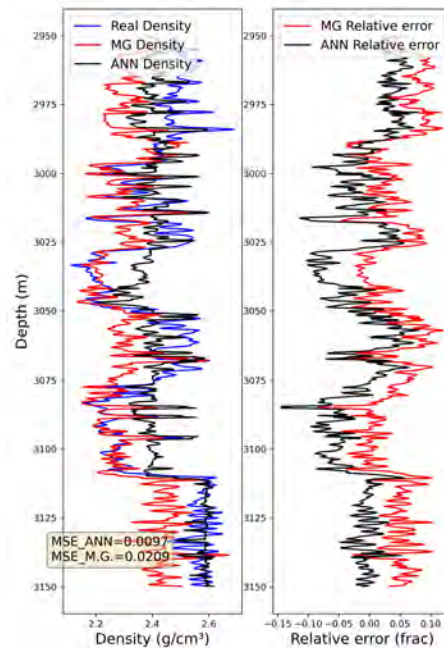
Similar tests were conducted comparing the modified Gardner’s equation with Oloruntobi and Butt (2019). The mean squared error was 0.0209 for the modified Gardner in a Campos Basin well log utilizing the parameters A, G, and m from Oloruntobi and Butt (2019). The parameters were calculated by non-linear regression from Norne field data. The mean squared error was 0.0355. Both results showed a larger error compared to the ANN model, which was 0.0097. These results are shown in Table 3. The correlation factors are displayed in Table 4 and Figures 8a and 8b show the adjusted curves and relative errors.

When the modified Gardner equation was applied to the Penobscot dataset utilizing the original parameters from the article, the mean squared error was 0.0105, while the parameters calculated by non-linear regression on a well log from Norne showed a mean squared error of 0.0099. Both errors were larger than the ANN model error, which was 0.0074. Figures 9a and 9b show the fits of the ANN and the empirical equations and their respective relative errors.

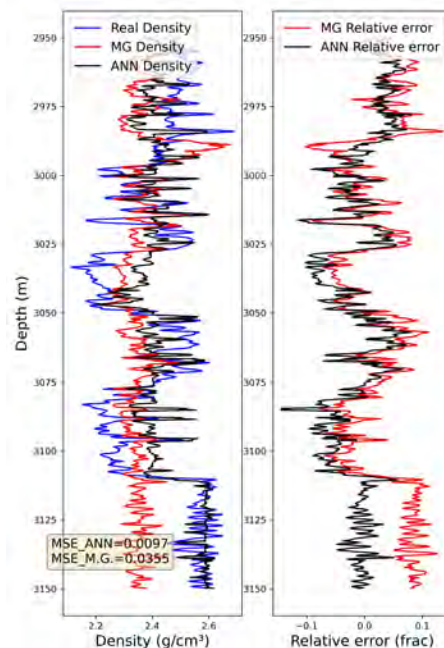
Figures 10a and 10b compare the empirical equations of Gardner et al. (1974) and of Oloruntobi and Butt (2019) with the second ANN model, which was trained with the P-wave velocity ( $V_P$ ), gamma-ray ( $GR$ ), and neutron porosity ( $\phi_N$ ) logs as input. The training data consisted of logs from the Norne, Penobscot, and Campos fields, and the ANN model was tested in a well from a different area of the Campos Basin. The ANN model presented a smaller MSE (mean squared error) and a smaller RMSE (root mean squared error), although these values were very close to the ones presented by the traditional Gardner model, as Table 5 shows. The modified Gardner model presented a larger error for this well log. The correlation factor (R) was closer to one for the ANN model, as Table 5 shows.

Table 5: MSE, RMSE and R values for the second ANN, the traditional Gardner, and the Modified Gardner models applied in a well log from the Campos Basin.

Model	MSE	RMSE	R
Second ANN	0.01001	0.10	0.73
Traditional Gardner	0.0105	0.1026	0.67
Modified Gardner	0.0263	0.1622	0.57

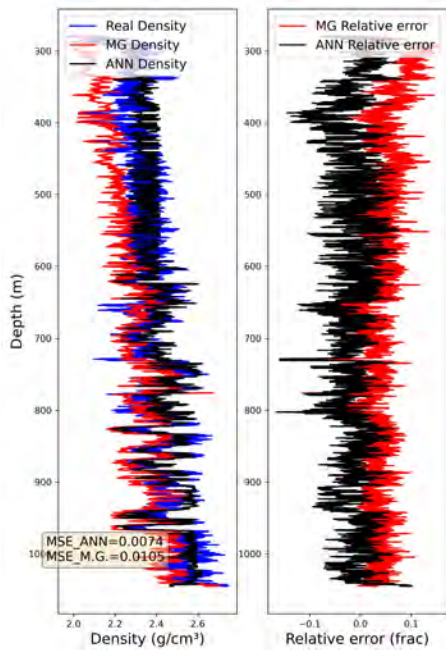


(a) Modified Gardner (A.V.).

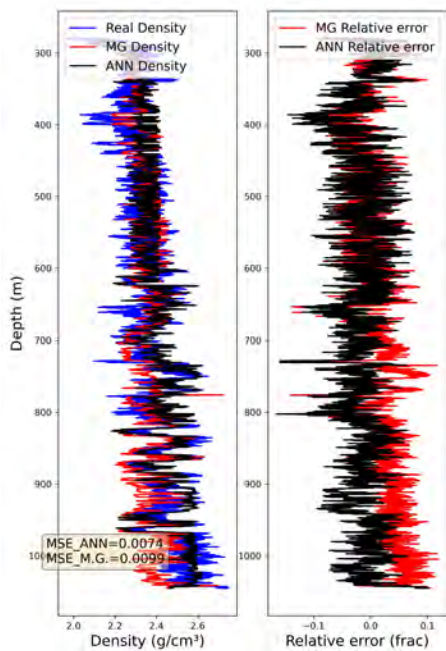


(b) Modified Gardner (INV).

Figure 8: Comparison between the fit of the density log constructed with the ANN and the modified Gardner model. (a) Here, it is the comparison of the modified Gardner model with its article parameter values (A.V.) represented by the red curve on the plot, and the density log constructed by the ANN model (black curve). (b) Here, it is the comparison of the modified Gardner model with its parameter values calculated in a Norne field well log by inversion (INV) represented by the red curve on the plot, and the density log constructed by the ANN model (black curve). Both are applied in a Campos Basin dataset.

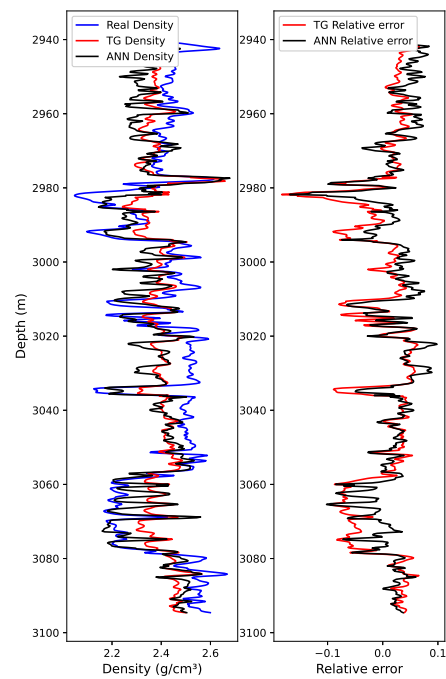


(a) Modified Gardner (A.V.).

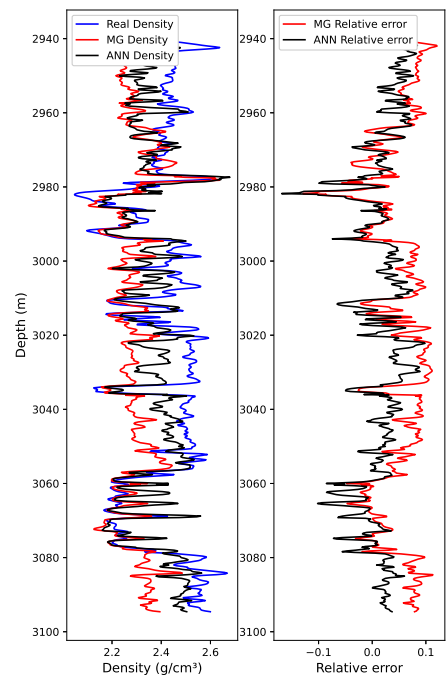


(b) Modified Gardner (INV).

Figure 9: Comparison between the fit of the density log constructed with the ANN and the modified Gardner model. (a) It compares the modified Gardner model with its article parameter values (A.V.), represented by the red curve on the plot, to the density log constructed by the ANN model (black curve). (b) It is a comparison of the modified Gardner model with its parameter values calculated in a Norne field well log by inversion (INV), represented on the plot by the red curve, and the density log constructed by the ANN model (black curve). Both are applied in the Penobscot dataset.



(a) Traditional Gardner (A.V.).



(b) Modified Gardner (A.V.).

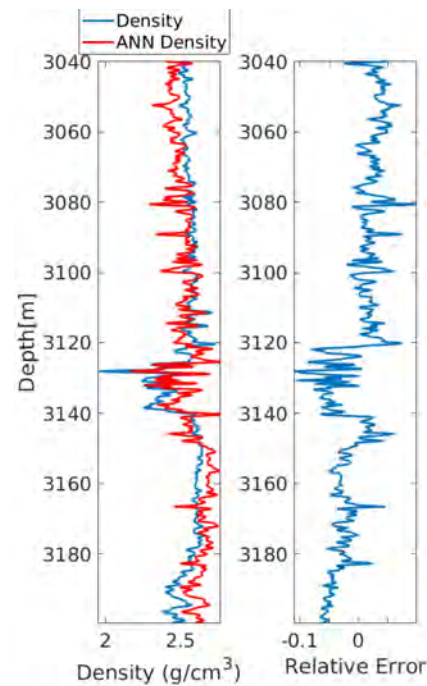
Figure 10: Comparison between the fit of the density log constructed with the ANN and the traditional Gardner model. (a) Compares the traditional Gardner model with its article parameter values (A.V.), represented by the red curve on the plot with the density log constructed by the second ANN model (black curve). (b) It is the comparison of the modified Gardner model with its article parameter values (A.V.), represented by the red curve on the plot, and the density log constructed by the second ANN model (black curve). Both are applied in the Campos Basin dataset.

## DISCUSSION

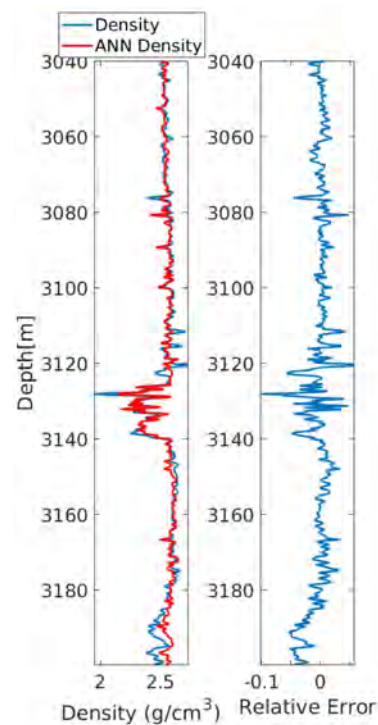
The original parameter values utilized in the empirical equations of Gardner et al. (1974) and of Oloruntobi and Butt (2019) were very close to the values obtained by linear and non-linear regression for the first dataset in this work that contains geologic information from very distinct sedimentary basins. However, both ANN models created in this work, tested with the same geologic data, showed smaller MSE values and correlation factor values closer to one. The empirical equations of Gardner et al. (1974) and of Oloruntobi and Butt (2019) had a good performance on constructing the density log by presenting a low MSE and a high Pearson's Correlation Coefficient. Nevertheless, when the equation parameters were obtained utilizing linear and non-linear inversion for a reference well from the Norne field data, the errors increased significantly, showing that the article parameters are a better option for the calculation.

It was possible to observe that, utilizing the equation of Oloruntobi and Butt (2019) with the parameters obtained by inversion in a Norne field well log, a good adjustment was presented when applied in the Penobscot field data, which might indicate that both fields have similar lithology composed of shaly rocks. For the comparison of the first ANN model with the empirical models on the Penobscot data, it is possible to observe in Figures 7b and 9a that, in depths ranging from 300 m to 650 m, the ANN model makes a much better adjustment with the real density curve than the empirical models; from 650 m to 1000 m, the ANN density and the modified Gardner density are close. However, it is possible to observe in the figure that the RE of the ANN model is close to zero while the RE of the modified Gardner (MG) model is closer to 10%.

For the Campos Basin well log, utilized on the tests for the comparison of the empirical models with the first ANN model, shown in Figures 6a and 8a, it is possible to observe that, from depths between 3095 m and 3110 m, the traditional Gardner and the ANN model do not make a good adjustment compared to the modified Gardner model, which might indicate a very shaly formation or a washout. However, for the rest of the well, for depths from 3110 m to 3150 m, for example, the ANN model makes a better adjustment than both empirical models.



(a)



(b)

Figure 11: (a) Comparison of the fit of the density log constructed with a third ANN model with the  $V_P$ ,  $V_{sh}$ , and  $\phi_N$  logs, as input data (red curve), and the measured density log (blue curve). Here, the training and application were made using the data from the Campos Basin. (b) A comparison of the fit of the density log constructed with a third ANN model with the  $V_P$ ,  $V_{sh}$ ,  $\phi_N$ , and ILD logs as input data (red curve), and the measured density log (blue curve). Here, the training and application of the data from the Campos Basin were also made.

The second ANN model was fed with less well log data, due to a lack of clean neutron porosity logs which were used as input; nevertheless, the second model also presented smaller MSE and RMSE compared to the empirical models and the R values were also closer to one. The performance of the second ANN model can be observed in Figures 10a and 10b, from depths equal to 2980 m to 3020 m, and from 3060 m to 3080 m. An additional ANN model was created using as input logs the P-wave velocity ( $V_P$ ), the shale volume fraction ( $V_{sh}$ ), and the neutron porosity ( $\phi_N$ ) with data from the Campos Basin utilized for training. The results for this simple ANN model are shown in Figure 11a. The MSE was equal to 0.01.

Figure 11b shows the results for a fourth ANN model very similar to the previous one but with a different additional resistivity (ILD) log. The MSE was equal to 0.006. Comparing the results from Figures 11a and 11b, it is possible to conclude that, by adding more log information to the training dataset, the error decreases and the model gets more accurate.

## CONCLUSION

When compared to empirical models, both ANN models had a better match for density log estimation, with reduced mean squared errors, root mean squared errors, relative errors, and higher Pearson's Correlation Coefficient. Our findings suggest that using ANN regression models to determine the density log for a wide range of sedimentary lithologies is a viable choice.

The adjustment of the ANN models does not fit the real density log in some regions of the wells due to several different geologic and tectonic factors, such as washout and mud filtrate, which affect the bulk density measurement and, consequently, the density adjustment of both empirical and ANN models. Nevertheless, as mentioned before, the statistical analysis showed that the ANN models outperform the empirical models on the wells where they were applied. On the comparison between the two empirical models, it was observed that there are some shaly formations where the modified Gardner model of Olorunjobi and Butt (2019) outperforms the traditional model of Gardner et al. (1974); however, both models presented good adjustments.

The two-layer neural networks constructed with 25 neurons on the first layer presented satisfactory results. For further studies, an ANN model might present an even better performance than the ones obtained in this work with a larger number of hidden layers on the ANN training algorithm and with a larger training dataset containing multiple well log data as input, such as caliper, electroresistivity, permeability, and many others, although it would greatly increase the computation time. It is something worth testing in future works.

## ACKNOWLEDGMENTS

This work was kindly supported by the Brazilian agencies INCT-GP and CNPq from Brazil and the Geophysics Graduate Program at Federal University of Pará. We also would like to thank the two reviewers and the editors for many helpful comments and suggestions and Maria Oliveira and Fernanda Moura for the help with some figures.

## REFERENCES

- Beale, M. H., M. T. Hagan, and H. B. Demuth, 2010, Neural network toolbox user's guide user's guide. MathWorks.
- Birch, F., 1960, The velocity of compressional waves in rocks to 10 kilobars: 1.: Journal of Geophysical Research, **65**, 1083–1102, doi: <https://doi.org/10.1029/JZ065i004p01083>.
- Brocher, T. M., 2005, Empirical relations between elastic wavespeeds and density in the Earth's crust: Bulletin of the Seismological Society of America, **95**, 2081–2092, doi: <https://doi.org/10.1785/0120050077>.
- Christensen, N. I., and W. D. Mooney, 1995, Seismic velocity structure and composition of the continental crust: A global view: Journal of Geophysical Research: Solid Earth, **100**, 9761–9788, doi: <https://doi.org/10.1029/95JB00259>.
- Clavier, C., W. Hoyle, and D. Meunier, 1971, Quantitative interpretation of thermal neutron decay time logs: Part I. fundamentals and techniques: Journal of Petroleum Technology, **23**, 743–755, doi: <https://doi.org/10.2118/2658-A-PA>.
- Gardner, G., L. Gardner, and A. Gregory, 1974, Formation velocity and density—the diagnostic basics for stratigraphic traps: Geophysics, **39**, 770–780, doi: <https://doi.org/10.1190/1.1440465>.
- Han, D.-h., A. Nur, and D. Morgan, 1986, Effects of porosity and clay content on wave velocities in sandstones: Geophysics, **51**, 2093–2107, doi: <https://doi.org/10.1190/1.1442062>.
- Hara, K., D. Saito, and H. Shouno, 2015, Analysis of function of rectified linear unit used in deep learning: 2015 International Joint Conference on Neural Networks (IJCNN), IEEE, 1–8.
- Hebb, D. O., 1949, The first stage of perception: growth of the assembly, in *The Organization of Behavior*: Wiley, New York.
- Kailath, T., 1980, *Linear systems*: Prentice-Hall Englewood Cliffs, NJ, 682.
- Kayri, M., 2016, Predictive abilities of bayesian regularization and Levenberg–Marquardt algorithms in artificial neural networks: a comparative empirical study on social data: *Mathematical and Computational Applications*, **21**, 20, doi: <https://doi.org/10.3390/mca2102020>.
- Kim, P., 2017, *Matlab deep learning with machine learning, neural networks and artificial intelligence*: Apress Berkeley, CA.

- (<https://doi.org/10.1007/978-1-4842-2845-6>).
- Kohli, A., and P. Arora, 2014, Application of artificial neural networks for well logs: IPTC 2014: International Petroleum Technology Conference, European Association of Geoscientists & Engineers, Doha, Qatar, 1–8.
- Leon, S. J., I. Bica, and T. Hohn, 1998, Linear algebra with applications: Prentice-Hall Upper Saddle River, NJ, 528.
- Levenberg, K., 1944, A method for the solution of certain non-linear problems in least squares: Quarterly of Applied Mathematics, **2**, 164–168, doi: <https://doi.org/10.1090/qam/10666>.
- Lindseth, R. O., 1979, Synthetic sonic logs—a process for stratigraphic interpretation: Geophysics, **44**, 3–26, doi: <https://doi.org/10.1190/1.1440922>.
- Long, W., D. Chai, and F. Aminzadeh, 2016, Pseudo density log generation using artificial neural network: Presented at the SPE Western Regional Meeting, Society of Petroleum Engineers, SPE-180439-MS.
- Lv, C., Y. Xing, J. Zhang, X. Na, Y. Li, T. Liu, D. Cao, and F.-Y. Wang, 2017, Levenberg–Marquardt backpropagation training of multilayer neural networks for state estimation of a safety-critical cyber-physical system: IEEE Transactions on Industrial Informatics, **14**, 3436–3446, doi: [10.1109/TII.2017.2777460](https://doi.org/10.1109/TII.2017.2777460).
- Marquardt, D. W., 1963, An algorithm for least-squares estimation of nonlinear parameters: Journal of the Society for Industrial and Applied Mathematics, **11**, 431–441, doi: <https://doi.org/10.1137/0111030>.
- McCulloch, W. S., and W. Pitts, 1943, A logical calculus of the ideas immanent in nervous activity: The Bulletin of Mathematical Biophysics, **5**, 115–133, doi: <https://doi.org/10.1007/BF02478259>.
- Menon, A., K. Mehrotra, C. K. Mohan, and S. Ranka, 1996, Characterization of a class of sigmoid functions with applications to neural networks: Neural Networks, **9**, 819–835, doi: [https://doi.org/10.1016/0893-6080\(95\)00107-7](https://doi.org/10.1016/0893-6080(95)00107-7).
- Oloruntobi, O., and S. Butt, 2019, The new formation bulk density predictions for siliciclastic rocks: Journal of Petroleum Science and Engineering, **180**, 526–537, doi: <https://doi.org/10.1016/j.petrol.2019.05.017>.
- Rochester, N., J. Holland, L. Haibt, and W. Duda, 1956, Tests on a cell assembly theory of the action of the brain, using a large digital computer: IRE Transactions on Information Theory, **2**, 80–93, doi: [10.1109/TIT.1956.1056810](https://doi.org/10.1109/TIT.1956.1056810).
- Rosenblatt, F., 1958, The perceptron: a probabilistic model for information storage and organization in the brain: Psychological Review, **65**, 386, doi: <https://doi.org/10.1037/h0042519>.
- Stigler, S. M., 1981, Gauss and the invention of least squares: The Annals of Statistics, **9**(3): 465–474., doi: [10.1214/aos/1176345451](https://doi.org/10.1214/aos/1176345451).
- Van der Baan, M., and C. Jutten, 2000, Neural networks in geophysical applications: Geophysics, **65**, 1032–1047, doi: <https://doi.org/10.1190/1.1444797>.
- Widrow, B., 1960, Adaptive switching circuits: IRE WESCON Convention Record, pt. 4, IRE, 96–104.
- Zeng, L., W. Ren, L. Shan, and F. Huo, 2022, Well logging prediction and uncertainty analysis based on recurrent neural network with attention mechanism and Bayesian theory: Journal of Petroleum Science and Engineering, **208**, 109458, doi: <https://doi.org/10.1016/j.petrol.2021.109458>.

**Carvalho, C.P.:** Code implementation, data gathering and organization, text writing, review and editing; **Silva, C.B.:** Idea conceptualization, text review and editing; **Figueiredo, J.J.S.:** Idea conceptualization, Code implementation, data gathering, text review and editing; **Carrasquilla, M.D.L.:** Geological review, organization and editing of figures, text review and editing.

Received on December 31, 2021 / Accepted on June 28, 2022



Creative Commons attribution-type CC BY